

Article

# A Novel Way of Adhering PET onto Protein (Wheat Gluten) Plastics to Impart Water Resistance

Oisik Das <sup>1,\*</sup>, Thomas Aditya Loho <sup>2</sup>, Antonio José Capezza <sup>1,3</sup>, Ibrahim Lemrhari <sup>1</sup> and Mikael S. Hedenqvist <sup>1,\*</sup>

<sup>1</sup> Department of Fibre and Polymer Technology, Polymeric Materials Division, School of Engineering Sciences in Chemistry, Biotechnology and Health. KTH Royal Institute of Technology, Stockholm 10044, Sweden; ajcv@kth.se (A.J.C.); bramslem@hotmail.fr (I.L.)

<sup>2</sup> Department of Chemical and Materials Engineering, The University of Auckland, Auckland 1142, New Zealand; thomas.loho@auckland.ac.nz

<sup>3</sup> Department of Plant Breeding, Faculty of Landscape Planning, Horticulture and Crop Production Sciences, Swedish University of Agricultural Sciences, Alnarp 23053, Sweden

\* Correspondence: oisik@kth.se or odas566@aucklanduni.ac.nz (O.D.); mikaelhe@kth.se (M.S.H.); Tel.: +46-790-469-886 (O.D.); +46-706-507-645 (M.S.H.)

Received: 9 October 2018; Accepted: 27 October 2018; Published: 31 October 2018



**Abstract:** This study presents an approach to protect wheat gluten (WG) plastic materials against water/moisture by adhering it with a polyethylene terephthalate (PET) film using a diamine (Jeffamine<sup>®</sup>) as a coupling agent and a compression molding operation. The laminations were applied using two different methods, one where the diamine was mixed with the WG powder and ground together before compression molding the mixture into plates with PET films on both sides. In the other method, the PET was pressed to an already compression molded WG, which had the diamine brushed on the surface of the material. Infrared spectroscopy and nanoindentation data indicated that the diamine did act as a coupling agent to create strong adhesion between the WG and the PET film. Both methods, as expected, yielded highly improved water vapor barrier properties compared to the neat WG. Additionally, these samples remained dimensionally intact. Some unintended side effects associated with the diamine can be alleviated through future optimization studies.

**Keywords:** PET; lamination; nanoindentation; water vapor barrier; interface

## 1. Introduction

The advent of the sustainability concept and the need for renewable materials has exposed wheat gluten (WG) as an attractive biopolymer [1]. The fact that WG is a by/co-product of the cereal processing industry, has good oxygen barrier properties in dry conditions, and is completely bio-based/biodegradable makes it an ideal candidate for propagating natural materials in the current polymer market [2]. WG possesses properties that make it suitable for replacing synthetic polymers in certain packaging, absorbent, and semi-structural applications [3]. WG can also be processed into films, foams, and solid 3D structures using extrusion, freeze-drying, compression, and injection molding [4]. Despite the aforementioned advantages of WG, there are certain inherent properties that adversely affect its applicability. WG is very susceptible to moisture and water [5], wherein the formed polymer can suffer from dimensional instability, inferior mechanical properties, microbial/fungal attack, and loss of barrier properties. If WG is intended to be used in e.g., food or medical packaging, it is critical in several cases that the polymer is resistant to moisture/water and has a low water vapor transmission rate. This would allow the moist food (e.g., cheese, cakes) to retain the required moisture and dry food (chips, fried, cookies) to remain crisp. Hence, the moisture resistance of the packaging material will

enhance the shelf life of the stored food [6]. Moreover, if WG is planned to be applied as semi-structural elements, it is important that the polymer does not lose its structural integrity due to plasticization and degradation by microbes/fungus (which thrive on moisture). Therefore, to preserve the application potential of WG, it has become necessary to impart moisture and water resistance properties [7].

Several studies have been conducted where it was attempted to bestow WG and its films with the necessary moisture and water vapor resistance. Researchers have performed studies to chemically modify WG using cross-linkers to render them moisture resistant [8–10]. In other studies, different types of coatings (lipids, oils, and hydrophobic polymers) have been applied onto the WG substrate to create water resistant layers [8,11]. In a study by Cho et al. [12], WG films were laminated with poly(lactic acid) (PLA) to improve their water vapor barrier properties. The PLA coating was applied through the process of compression molding and the authors observed that the water vapor transmission rate (WVTR) was reduced irrespective of the content of glycerol in the WG film. However, the interlayer adhesion was deteriorated as a result of increased WG molding temperature (ca. 130 °C). Irissin-Mangata et al. [2] applied a UV-cured coating (hydrophobic cross-linked photopolymer) on WG films using a wire-wound applicator to render it moisture resistant. It was reported that the coating was able to decrease the water vapor transmission rate of the WG films. However, the study only visually analyzed the adhesion of the coating with the WG through scanning electron microscopy (SEM), and no quantitative measurement of the adhesive strength of the coated layer was presented. In an earlier study by the same authors [13], functionalized polyethylene films (ethylene/acrylic ester/maleic anhydride terpolymer and ethylene/glycidyl methacrylate copolymer) were compression molded onto a WG substrate. Although both coatings were able to reduce the water vapor transmission rate, only the terpolymer adhered to the WG film. The authors presented no quantitative measurements of the adhesion of the coating with the WG. Most probably, the adhesion of the terpolymer was due to the formation of covalent bonds, but the authors cited Van der Waal forces and hydrogen bonds as possible reasons.

Different types of hydrophobic lipids have also been applied (added to the film-forming solution) on WG films to provide water resistance [14]. It was observed that beeswax performed the best (amongst the tested lipids) to enhance the moisture barrier properties. However, the coating of the beeswax lipid reduced the transparency of the WG films while also exhibiting low puncture strength and a tendency to easily disintegrate in water. In another study by Gontard et al. [8], a thin layer of lipid was deposited (i.e., coated) onto WG films to create a water vapor barrier. Similar to the earlier study, beeswax and paraffin wax were reported to induce the highest improvement in the water vapor barrier properties. Nevertheless, the authors met with challenges since the hydrophilic WG under-layer expanded and fractured the brittle lipid layer when water reached this phase. Moreover, aside from being brittle, the lipid coating suffered from poor adhesion to the WG and oxidative instability. Fabra et al. [15] were able to reduce the water permeability of WG significantly (by ca. 88%) using a coating of annealed polyhydroxybutyrate electro spun fibers. The coated sample also exhibited a contact angle of 70°. Despite enhancing the barrier and mechanical properties, the color of the WG films turned brown and translucent. Elsewhere, Micard et al. [16] unsuccessfully endeavored to reduce the vapor permeability of WG films by chemical (formaldehyde vapors) and physical treatments (temperature and radiation). From the above-mentioned studies, it can be stated that most of the layers applied to WG lacked the proper adhesion (or its experimental determination thereof) while changing the appearance of the WG. This necessitates the exploration of other layering agents with reduced water transmission that can adhere strongly to WG with the aid of a coupling agent (preferably already used in treating WG polymers).

The central idea for the current study was obtained unintentionally. Jeffamine, a diamine, was tested for chemically cross-linking WG for the same purpose of rendering it more water resistant. While molding the WG sample (with the added diamine) using the hot press, polyethylene terephthalate (PET) films were used instead of the usual Teflon films. It was observed that post compression molding, the PET films were strongly attached to the WG sample, which indicated that the diamine acted

as a coupling agent, reacting with both the PET layer and the WG polymer. The strongly adhered PET layer would impart the necessary water resistance, ensuring the preservation of the high oxygen barrier properties of the WG component, similar to how high oxygen barrier properties are preserved for the ethylene vinyl alcohol (EVOH) layer when surrounded by polyethylene or polypropylene layers in food packaging. It has to be kept in mind though that the addition of PET to WG would reduce the sustainability aspect to some extent. However, bio-based PET is an upcoming material that is being increasingly researched [17] and holds potential to be used in the market soon. Therefore, this study lays the foundation for the application of PET, bio-based or otherwise, on WG plastics to impart water vapor barrier properties. The PET layered WG can be separated for recycling since WG is biodegradable and PET is not. Hence, for example, after the WG has degraded (facilitated by cutting the material into pieces to expose the WG for its decomposition), the PET can be recycled to form rPET (post separation from decomposed WG). More importantly, the research and development of bio-based plastics, like WG, should not be affected by the recycling landscape. Alaerts et al. [18] stated that if the bio-based plastics could be recycled on their own, the entire recycling landscape would be able to accommodate them eventually.

The overarching aim of this study was to apply a PET layer onto the WG polymer surface through two different methods and test their nanomechanical and water vapor resistance properties. Changes in the microscopic, chemical, and macro-mechanical properties as a result of the PET application were also evaluated accordingly. Since most of the previous studies did not attempt to definitively and quantitatively measure the adhesion properties of the coating with the WG, the current study employed the nanoindentation technique. Nanoindentation provided a new way to comprehend the nature of the adhesion of the PET layer to the WG component by determining the nanohardness and nanomodulus in the interfacial PET/WG region. In addition to the nanoindentation approach, the novelty of the work also lies in the method of using a diamine to laminate WG with a more water resistant layer (here PET).

## 2. Materials and Methods

### 2.1. Manufacturing of the Samples

The PET layer was applied on to the WG material (supplied by Lantmännen Reppe AB of Stockholm, Sweden with a gluten protein content of 77.7 wt %) using two different application methods. The first method involved compression molding (Fortijne Presses TP 400, Barendrecht, Netherlands) WG powder at 150 °C for 30 min at 290 kN force. Next, 15 wt % of Jeffamine (Jeffamine EDR 148 procured from Huntsman Corporation, Göteborg, Sweden) was brushed onto the molded WG surface and then compression molded again with the initially 250 µm thick PET films (Mylar<sup>®</sup> A, Synflex Insulation Systems, Blomberg, Germany) using the same pressing conditions. The amount of Jeffamine added was decided based on previous studies [19,20]. This sample was named “Brushed” since the Jeffamine was applied externally. In the other application method, 15 wt % Jeffamine was first added to the WG powder, then mixed through dry blending. This was followed by flash freezing in liquid N<sub>2</sub> and grinding (Retsch GmbH, 5657, Haan, Germany). The WG powder containing the Jeffamine was then compression molded along with the PET sheets using the same pressing conditions as mentioned previously. This sample was named “Ground”. The neat WG sample (as the control) was also manufactured using the same process as for the “Ground” sample, but without the Jeffamine. The mold dimension was 100 × 100 × 4 mm<sup>3</sup>, thereby yielding samples of the same sizes. The PET layer was attempted to be forcibly and manually removed to qualitatively gauge its adhesion. It was observed that the PET was completely stuck to the WG polymer. For the WVTR measurements, the mold was circular with a diameter of 70 mm and a thickness of 1 mm. The PET layers were applied to both sides of the samples.

## 2.2. Testing of the Samples:

The tensile strengths and moduli (chord moduli between 0.05% and 0.25% strain) of the laminated and control samples were determined on an Instron Universal Testing Machine (10 kN load cell) (Model No. 5566, Instron, Norwood, MA, USA), using specimens that were 4 mm (the WG part) thick, 12.7 mm wide, and 100 mm long. The samples were milled out from the produced plates. The gauge length was 50 mm and the crosshead speed used was 50 mm/min, following the ASTM D638 Protocol [21].

Three top-down samples and three cross-sectional samples were prepared for nanoindentation in this study. The top-down samples were cut into squares with a ca. 15 mm side length and the cross-sectional samples were cut into squares with a ca. 10 mm side length using a SiC cut-off wheel (Struers, Cleveland, OH, USA). The cross-section of the cross-sectional samples was ground with 240 and 600 grit-size SiC abrasive papers (Struers) and polished with a 6  $\mu\text{m}$  diamond suspension (Struers). All samples were then cleaned with ethanol and fixed onto a mild steel plate using a cyanoacrylate adhesive. Figure 1 shows the orientation of the samples for the nanoindentation tests.

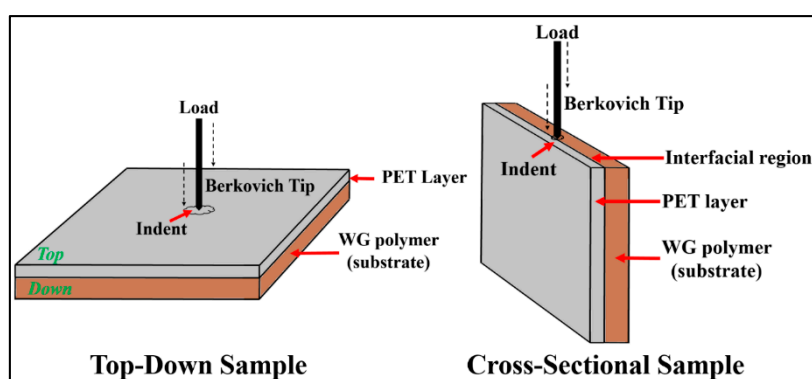


Figure 1. Sample orientation for nanoindentation.

The nanoindentation procedure was performed using a Hysitron TI950 TriboIndenter (Bruker, Billerica, MA, USA) at the University of Auckland, New Zealand. For both procedures, a 1  $\mu\text{m}$  diamond conical tip, commonly used for the nanoindentation of non-metallic materials, was used. On the top-down samples, five sets of nine standard quasi-static indents (5 s loading, 2 s holding, and 5 s unloading) with increasing maximum loads from 1000 to 9000  $\mu\text{N}$  were done at five random locations on the surface of the PET layer. On the cross-sectional samples, two sets of nine indents with a fixed maximum load of 5000  $\mu\text{N}$  were done at the interfacial region of the PET layer and the WG substrate. The hardness and modulus were calculated from the load-displacement data and the details are available elsewhere [22].

The WVTR of the samples were determined using 25  $\text{cm}^2$  VF2201 permeability cups from TQC. The cups, with a volume of 20 mL water, were fitted with the circular samples (exposing 25  $\text{cm}^2$  of the film to water vapor) and then placed in a room with 50% relative humidity at 23  $^{\circ}\text{C}$ . The mass loss due to water vapor transmission was measured according to ASTM D1653 protocol [23]. The water vapor transmission rate was calculated based on the water loss data between the third and fourth day.

A goniometer (CAM 200, KSV Instruments Ltd., Espoo, Finland) was used wherein a droplet of distilled water was placed on the flat surface of the sample and its contact angles were measured.

Fourier transform infrared spectroscopy (FT-IR) of the samples was performed in ATR mode on a Perkin Elmer Spectrum 100 instrument, Waltham, MA, USA. The layered samples were placed over the crystal to comprehend the chemical changes in that region. For each sample, 64 scans were obtained and averaged from the 600 to 4000  $\text{cm}^{-1}$  wavelength with a resolution of 4  $\text{cm}^{-1}$ . The scanning electron microscopy (SEM) of the tensile fractured samples and of the interfacial (PET/WG) regions were conducted on a Hitachi TM 100 table top SEM, Tokyo, Japan (10 kV voltage, 6 mm working distance). All the tests mentioned in this manuscript were performed in replicates (tensile tests had five

replicates, WVTR had two replicates, and the goniometer had ten replicates). The standard deviation measured was reported in the error bars of the figures and as numeric values in the table.

### 3. Results and Discussion

#### 3.1. Mechanical Properties

##### 3.1.1. Tensile Properties

The tensile properties of the laminated samples and the neat sample are summarized in Table 1. It can be observed that the neat WG had the highest tensile strength amongst the tested samples. Its tensile strength value of ca. 29 MPa is similar to that of the tensile strength of neat polypropylene [24], which is an important economic consideration. It is an essential first step in developing bio-based plastics that have the same tensile strength as a common and popular synthetic polymer (here polypropylene). The processing condition for the compression molding was decided after trial tests and a pressing temperature of 150 °C for 30 min was the most desirable in terms of good adhesion between PET and WG, and good cohesion of the WG matrix (enabled through sufficient melting during the molding cycle). It should be noted that a polyethylene film was also tested for adhesion to WG, but the effect observed with PET was absent. It was also observed that without pressure during the molding operation and without the diamine, the adhesion between PET and WG was absent. In addition, the particular processing condition enabled a heat-induced cross-linking (disulfide cross-linking) of the gluten network, which is known to enhance the mechanical strength of WG-based materials [25,26].

The addition of the diamine to WG caused some changes in the protein, which consequently reduced the tensile strength, ductility/strain at break and toughness. The effects were largest for the sample where the diamine had been mixed with the WG (Ground) and less for the sample with the diamine applied (Brushed) at the WG surface. It is known that at high temperatures, nitrogen-containing compounds such as diamine depolymerize polymers that possess amide groups [27]. The modulus, however, did not decrease in the presence of the diamine. An estimation of the laminate modulus employing the rule of mixtures for parallel geometry (using the neat WG modulus, Table 1 and PET modulus, 2.7 GPa) gave an unrealistically low value compared to those in Table 1. This revealed that the modulus of the WG component was higher in the presence of diamine due to the cross-linking [22,28]. During the tensile testing, no delamination of the PET layer was observed in any of the samples, which reaffirmed the fact that the bonding of PET to the WG polymer was strong. The results showed that in terms of mechanical properties, the brushing method was superior to the diamine/WG mixing (Ground) method. It should be noted though that both the Brushed and the Ground materials had sufficient mechanical properties for many applications (e.g., packaging, encapsulation of pest- or weed-control agents, toys, covers, frames for electrical devices, household appliances, and furniture) [13,29].

**Table 1.** Tensile properties.

Sample	Tensile Strength (MPa)	Tensile Modulus (GPa)	Strain at Break (%)	Toughness (J)
Neat WG	29.2 ± 2.1	1.2 ± 0.1	3.3 ± 2.3	1.36 ± 0.84
Ground	5.0 ± 1.6	1.3 ± 0.2	0.8 ± 0.4	0.04 ± 0.03
Brushed	17.3 ± 2.3	1.7 ± 0.3	2.3 ± 0.9	0.22 ± 0.04

##### 3.1.2. Nanoindentation

The use of the nanoindentation technique has been previously proven to be effective in evaluating the interfacial (amongst other) properties of polymer composites [22,30,31]. Therefore, in this study, the same technique was applied to determine the nanomechanical properties of the PET laminated and neat WG samples (sample thickness of 4.2 mm). Figures 2 and 3 show the nanomechanical hardness

and reduced modulus of the tested top-down samples, respectively. The hardness was essentially independent of the depth of the indentation and on the same level for both PET-layered WG samples, which was expected as the indentation was always in the PET layer. The indentation depth ranged from ca. 300 nm (for a 1000  $\mu\text{N}$  load) to 2000 nm (for a 9000  $\mu\text{N}$  load). This result suggests that the measured hardness was that of the PET with little to no substrate effect(s). For neat WG, there seemed to be a small but consistent increase in hardness inwards into the sample, however, based on standard deviation, the values were not significantly different.

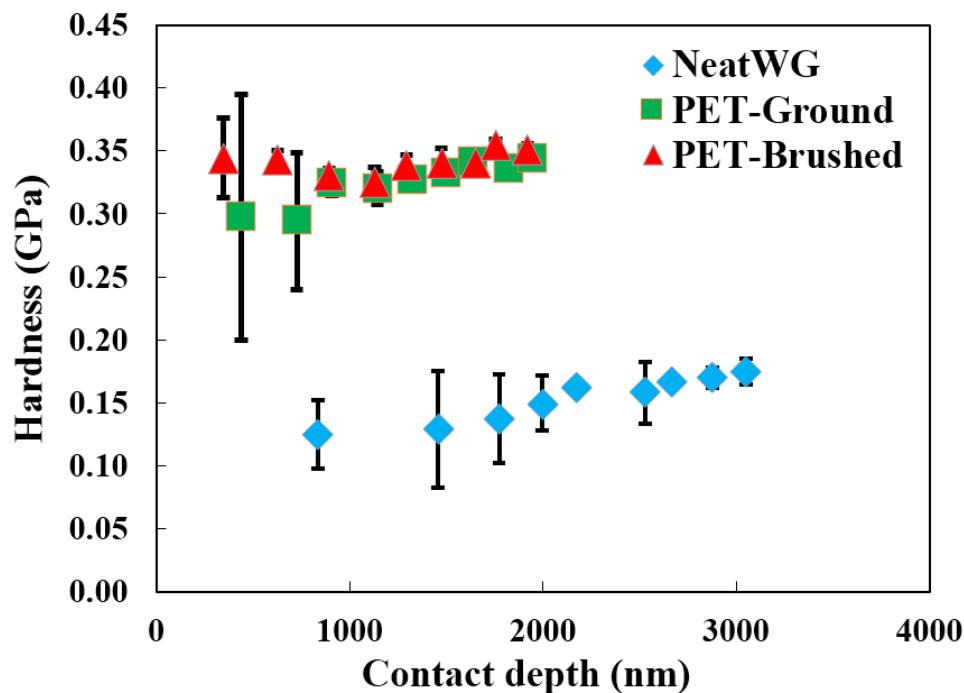


Figure 2. Nanoindentation hardness measured top-down.

From Figure 3, it can also be observed that the reduced modulus for neat WG increased with increasing depth, while the reduced modulus for the PET-layered samples remained depth-independent. Evidently, on a submicron to micron-range, the WG surface was less stiff than the interior, but still at a level comparable to that of the PET layer. From the nanoindentation hardness and reduced modulus values, it can be stated, that although the use of the diamine could have some adverse effects on the tensile strength and extensibility (see Section 3.1.1), the PET layers could increase the wear resistance of the samples, which is desirable (Figure 4). The wear resistance can be calculated as the ratio of the nanoindentation hardness to the modulus [32]. Figure 4 shows that the laminated samples had a significantly higher wear resistance when compared to that of the neat WG, and that the wear resistance of the laminated samples were the same.

The load vs. displacement curves of the samples tested top-down are presented in Figure 5. The unloading curves did not overlap the loading curves due to energy loss (damping) and a certain degree of plastic deformation. These effects were similar for the two PET-layered plates, but larger for the neat WG. Figure 6 shows the nanoindentation scan area of the top-down tested samples where the impression left after the conical-tip had indented the samples is clearly visible. This shows that the samples had deformed not only elastically, but also plastically, as also observed in Figure 5. Additionally, we noticed that the PET surfaces were flatter/smoother when compared to the WG material, implying a more elastic surface.

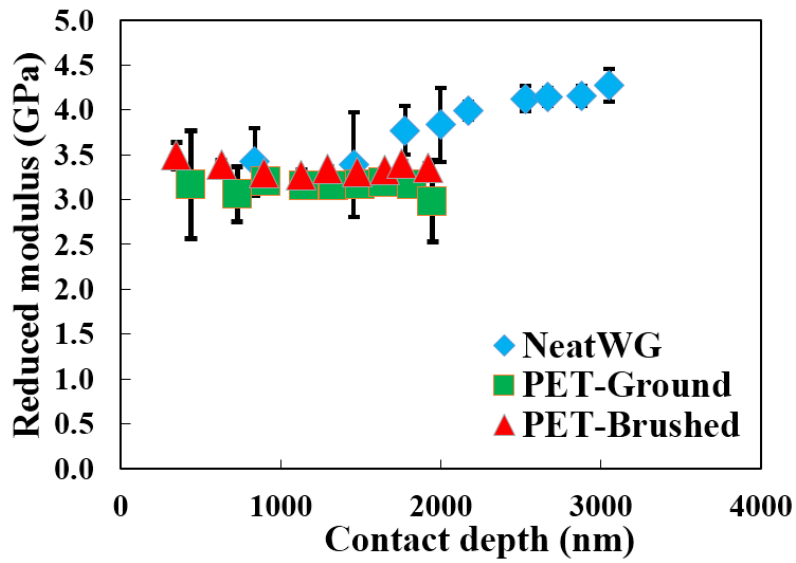


Figure 3. Reduced nanoindentation modulus measured top-down.

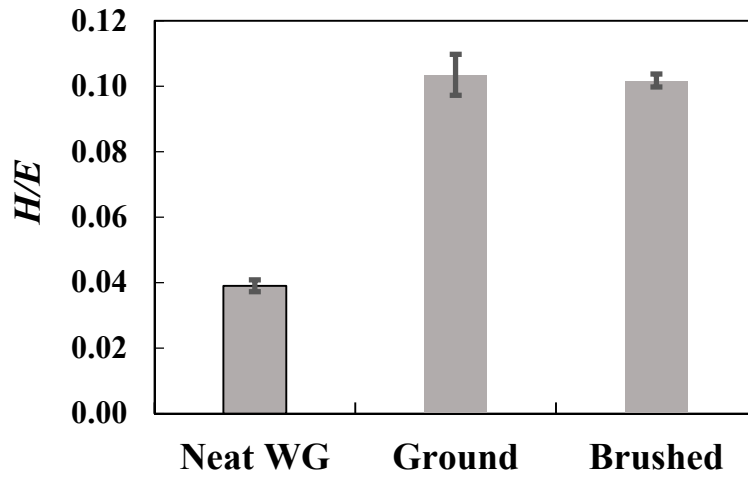


Figure 4. Wear resistance measured top-down.

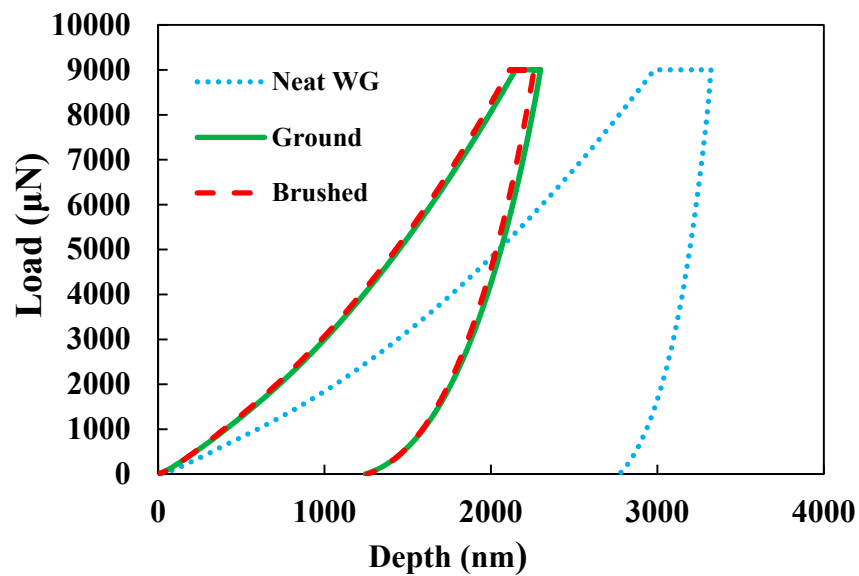
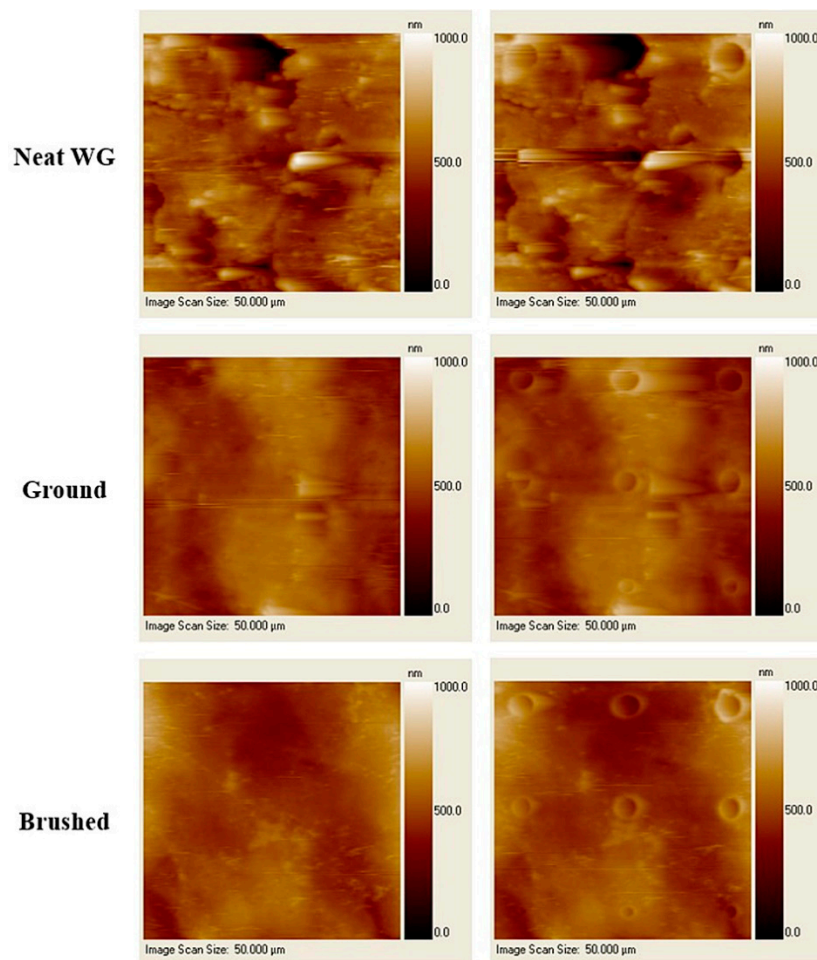


Figure 5. Load vs. displacement curves measured top-down.



**Figure 6.** Nanoindentation regions (before and after indentation) measured top-down. The width of 50  $\mu\text{m}$  in the images are the lateral dimension ( $x$ - $y$  axes). The color bar to the right of each image represents the height of the sample surfaces.

To comprehend the mechanical properties of the interface between the PET and WG, the samples were also analyzed by nanoindentation in the cross-section. The nanomechanical properties of the interfacial region are critical to gauge the nature of the adhesion of the laminations. The nanoindentation regions of the cross-sectional specimens are displayed in Figure 7 (optical image). Figure 8 shows that the hardness of the area containing the interface of the Ground sample (0.18 GPa) was similar to that of the neat WG (0.19 GPa) and the PET (0.21 GPa). The area containing the interface of the Brushed sample had a significantly lower hardness (0.07 GPa) than the corresponding area of the Ground sample. The reduced modulus (Figure 9) was also significantly lower in the area containing the interface of the Brushed sample. Hence, the interface of the Brushed sample was both weaker and less stiff than in the Ground sample. This suggests that the adhesion between the PET layer and WG was stronger in the Ground sample when compared to the Brushed sample. This can be attributed to the method of PET application that created a higher cross-link density. In the Brushed sample, the PET was in direct contact with the diamine, which had an aminolytic effect, resulting in the loss of PET structural integrity (see Sections 3.4 and 3.5).

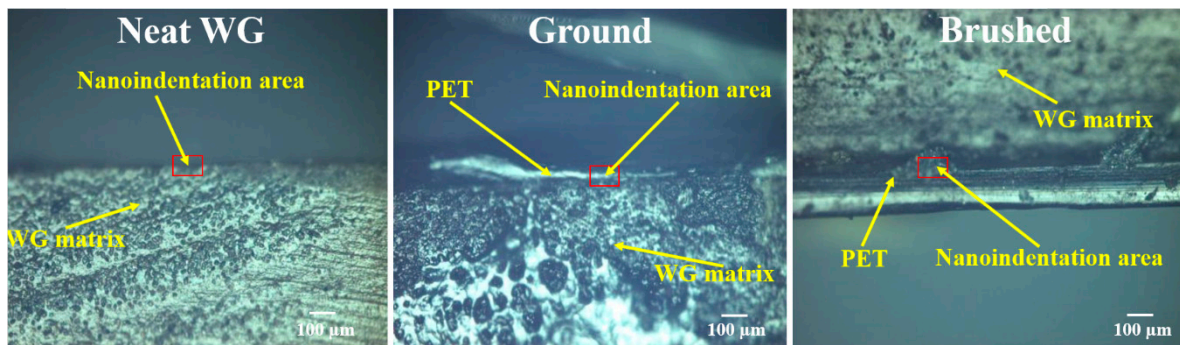


Figure 7. Nanoindentation regions of the cross-sectional samples.

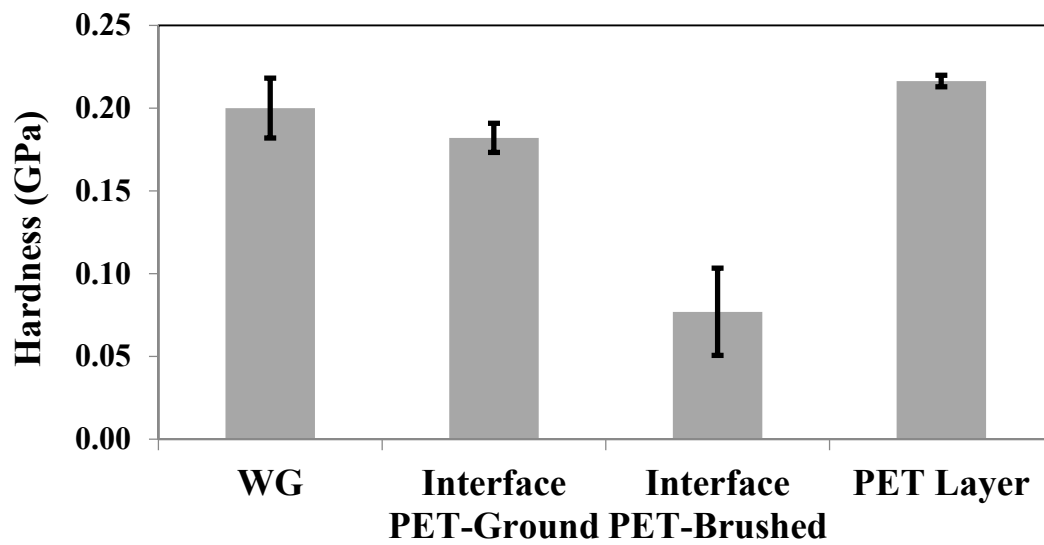


Figure 8. Nanoindentation hardness of the cross-sectional samples.

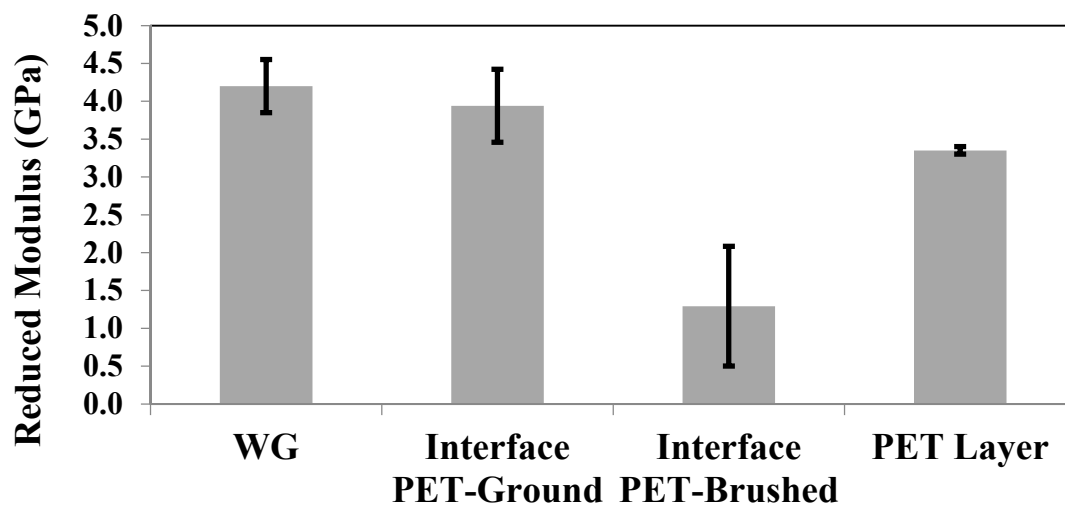


Figure 9. Nanoindentation modulus (reduced) of the cross-sectional samples.

### 3.2. Resistance Towards Water and Its Vapor

#### 3.2.1. WVTR Tests

The water mass loss curves during the permeation measurement are given in Figure 10. The initial slow loss of water in the case of the WG film was due to an extensive uptake of water vapor in the

film. Figure 11 shows how the initially flat film expanded and deformed during the test. The WVTR of the WG film (1 mm thick) was  $79.1 \pm 10.7 \text{ g}\cdot\text{m}^{-2}\cdot\text{day}^{-1}$  (calculated between the third and fourth day). The WVTR of the neat PET film was, as expected, significantly lower:  $11.2 \pm 0.6 \text{ g}\cdot\text{m}^{-2}\cdot\text{day}^{-1}$ . The Ground sample had a WVTR of  $15.6 \pm 4.2 \text{ g}\cdot\text{m}^{-2}\cdot\text{day}^{-1}$  that was similar to the neat PET film value (within the standard deviation). The measured WVTR of the brushed sample was, however, higher ( $23.3 \pm 4.9 \text{ g}\cdot\text{m}^{-2}\cdot\text{day}^{-1}$ ). The water vapor transmissions normalized to (WVTR values  $\times$  total PET thickness) the actual PET thickness were  $2800 \pm 150$ ,  $3060 \pm 820$ , and  $4570 \pm 960 \text{ g}\cdot\mu\text{m}/(\text{m}^2\cdot\text{day})$  for the neat PET, Ground, and Brushed samples, respectively. It was noted that there was a reduction in the total thickness (on both sides) of the PET (resulting thickness:  $(98 \pm 5) \times 2 = 196 \mu\text{m}$ ) in the pressed material when compared to that of the neat PET (250  $\mu\text{m}$ ). The somewhat higher transmission rate of the Ground sample could be attributed to the change in the layer thickness. The changes in PET thickness were probably not the cause for the higher WVTR of the Brushed sample. It is more likely that the increase in WVTR was due to the migration of the diamine into the PET under the hot pressing. Not all diamine reacted with the PET (or the WG) and this low molar mass component may serve as an internal plasticizer of the PET component. In addition, the diamine increased the hydrophilicity of the PET layer. The migration was obviously higher for the Brushed samples as all the diamine was already available at the WG–PET interface, whereas it needed to migrate from the matrix to the PET in the Ground samples. Nevertheless, the Ground sample showed an almost 80% reduction in WVTR whereas the Brushed sample showed a reduction of 70% (compared to neat WG).

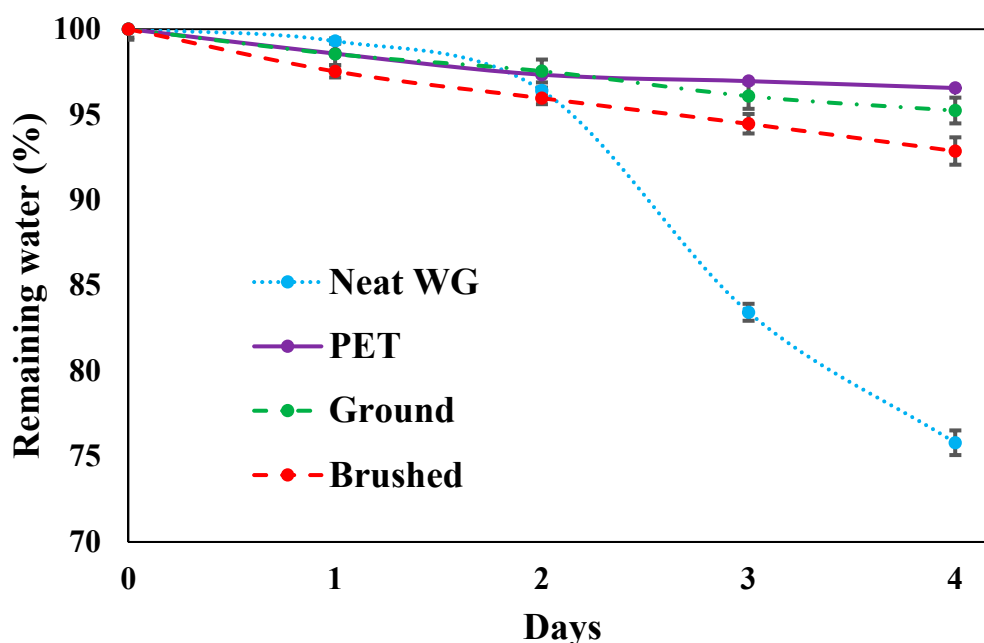
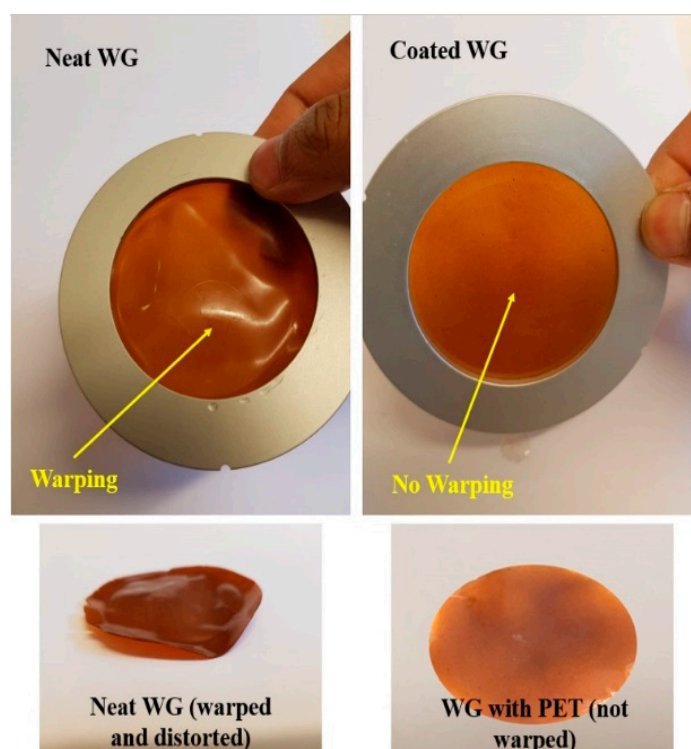


Figure 10. Water content inside the cup as a function of time.



**Figure 11.** State of the neat and PET-layered WG film when exposed to saturated water vapor (100% RH) on the inside of the cup and 50% RH on the outside.

### 3.2.2. Contact Angle

The low contact angle at the outer PET-layered surface of the Brushed plate ( $35^\circ \pm 4^\circ$ ) verified that the polar and hygroscopic diamine had penetrated the entire PET layer (Figure 12). The PET film had a contact angle of  $90^\circ \pm 1.2^\circ$  and the more polar WG film had a value of  $64^\circ \pm 1^\circ$ . The value of the PET-layer on the Ground sample was  $68^\circ \pm 2.5^\circ$ . A possible explanation for this lower value compared to the neat (un-pressed) PET film may be because the PET film surface becomes slightly oxidized/hydrolyzed during the pressing operation, however, on a level small enough not to be observed by IR spectroscopy (see below).

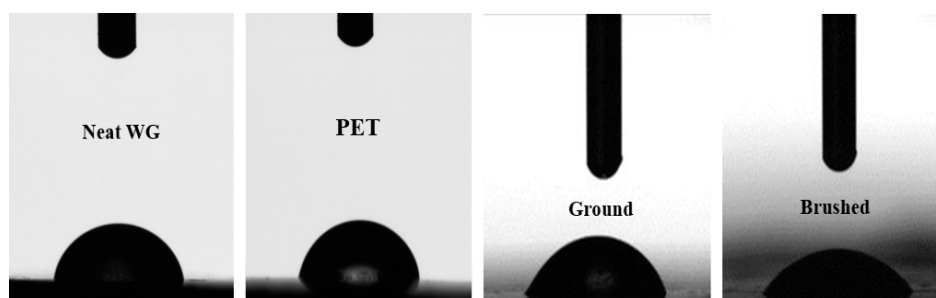


**Figure 12.** Water droplets on the samples during the goniometer test.

### 3.3. Infrared Spectroscopy

Figure 13 shows that the infrared (IR) spectrum of the Ground sample (measured top-down) was similar to that of the neat PET, showing that no diamine was present in the PET outer surface. The relative size of the PET ester peak ( $1712\text{ cm}^{-1}$ ) to that of the reference peak (ca.  $1410\text{ cm}^{-1}$ , phenylene-ring vibration) [33] was also the same (3.3) as that of un-pressed (neat) PET, indicating that the oxidation or hydrolysis of the PET layer was low enough not to be observed in the IR spectrum.

On the other hand, the spectrum of the PET layer of the Brushed sample showed a more pronounced absorbance in the 2800–3000  $\text{cm}^{-1}$  region than that of neat PET due to the presence of the diamine. The 1712/1410 peak ratio was also lower (2.7) than those in the un-pressed PET and Ground samples, indicating a reaction between the diamine and PET.

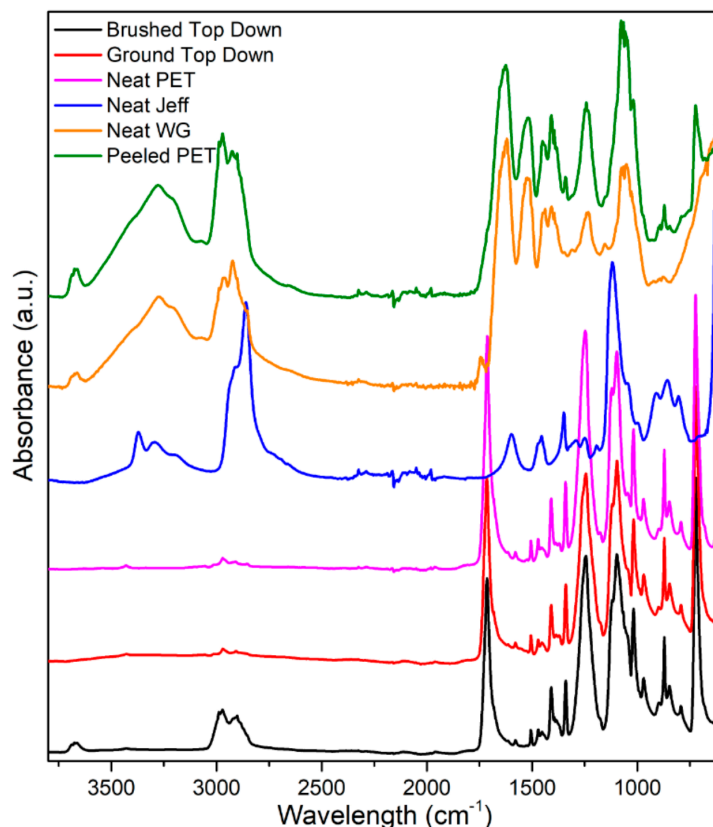


**Figure 13.** FT-IR spectra of the different neat components and the PET laminated WG.

In order to assess the strength of the bonding between the PET and WG, an attempt was made to peel off the PET layer from the WG and to run IR on the side of the layer that had faced the WG material. Figure 13 reveals that the inner surface (i.e., Peeled PET) showed clear features of WG (observed by the large amide I peak at 1700–1580  $\text{cm}^{-1}$ ). Additionally the  $\text{NH}_2/\text{OH}$  regions in the peeled PET was higher than that of the neat PET. This shows that during the peeling, the fracture went mainly through the WG material and not the PET/WG interface, which indicated a good bond between the PET and WG. Note also that this was the laminated WG with a weakest interface, i.e., the Brushed sample (weaker than that of the Ground sample).

#### 3.4. Microscopy (SEM)

Figure 14 shows the cross-sections of the outer regions of the tensile fractured surfaces of the PET layered WG materials. Notable is the “intact” interface between the WG and the PET layer in the Ground sample. In the Brushed sample, the cross-section was rougher than that of the Ground sample, indicating a less brittle sample in accordance with the tensile properties given in Table 1. Contrary to the Ground sample, a damaged interface could be seen in the Brushed sample. This observation corroborates the results of the cross-sectional nanoindentation, contact angle, and WVTR tests. Due to the better interfacial bonding of the PET to the WG polymer in the Ground sample, it had higher interfacial hardness and better water vapor barrier properties. Moreover, the PET layer in the Ground sample seemed to retain its structural integrity during fracture whereas the same in the Brushed sample was lacking. The PET layer in the latter exhibited extensive cracks. This was the

result of the direct contact of the PET layer with the diamine, which caused aminolysis of the PET (see Section 3.5). Consequently, the Brushed sample had inferior barrier properties when compared to the Ground sample.

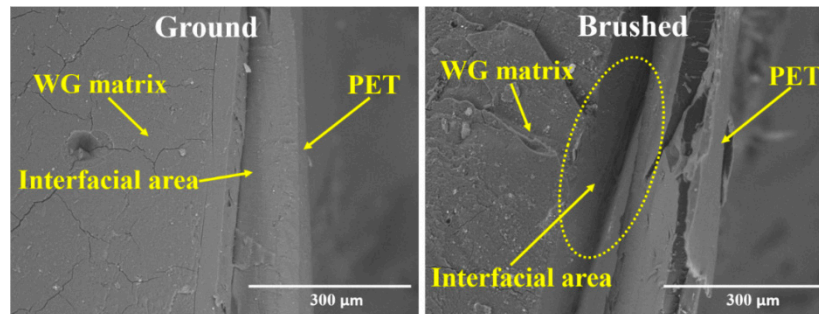


Figure 14. SEM micrographs of the tensile fractured surfaces.

### 3.5. Mechanisms of the Effects of the Diamine

Figure 15 illustrates the aminolysis of PET using a diamine [34], where the reaction led to a decrease in the PET molar mass. However, the amine terminated PET chain could react further with a second component (WG or another PET chain). Based on the IR data, it was observed that the ester groups of the PET reacted with the amine (decrease in the ester peak in the PET component of the Brushed sample). The good bond between WG and PET indicated that the un-reacted amine on the “aminated” PET reacted with WG at the interface. The presence of the diamine is a prerequisite for any bonding to occur at all between PET and WG. However, at high temperature, depolymerization involving amide containing polymers occurs in the presence of diamine [27]. Hence, the diamine reacts with the main chain protein amide causing a cleavage of the protein chain. Cross-linking reactions with the diamine as a coupling agent may also occur between the protein chains, however, the cleavage mechanism seems to dominate.

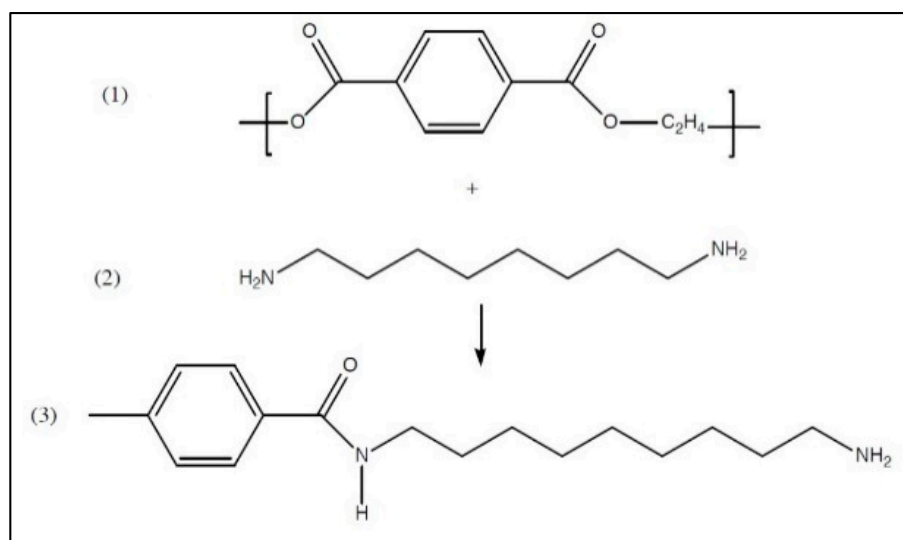


Figure 15. Aminolysis of PET.

## 4. Conclusions

Through the current study, an innovative step has been taken to apply a continuous, strong, and transparent layer aided by a coupling agent on WG plastics to impart water resistance. The diamine cross-linker (i.e., Jeffamine) that was used created a strong bond between the WG polymer and the

PET layer. The two methods used to laminate the protein plastic with PET had different advantages and drawbacks. In the Ground method, the strongest WG/PET interface was obtained but the protein was to some extent negatively affected (lower strength). The lower strength was due to the bulk WG material and not related to the adhesion with the PET layer. No delamination occurred between the WG and the PET layer in the Ground or the Brushed samples. In the Brushed method, the protein was less affected, but the interfacial strength and the hydrophobicity of the PET layer, containing migrated diamine, was lower, also leading to a somewhat poorer water vapor transmission rate. Nevertheless, both methods of lamination with PET led to significantly higher water vapor barrier properties than that of neat WG. The PET layered samples also remained undistorted during the water exposure. One of the biggest issues with WG is its dimensional instability under high humidity conditions. The PET layers, having a strong adherence to the WG, eliminated this issue. Still, there is room for improvement regarding the negative side-effects of the diamine and future work should include the optimization of the content of the added diamine as well as the processing conditions.

**Author Contributions:** Conceptualization, O.D. and M.S.H.; Methodology, O.D. and M.S.H.; Formal Analysis, O.D., T.A.L., and A.J.C.; Investigation, O.D. and I.L.; Data Curation, O.D., T.A.L., A.J.C., and M.S.H.; Writing—Original Draft Preparation, O.D.; Writing—Review & Editing, O.D., T.A.L., A.J.C., and M.S.H.; Supervision, O.D. and M.S.H.; Project Administration, M.S.H.; Funding Acquisition, M.S.H.

**Funding:** This research was funded by the Lantmännen Research Foundation (No. 2016H010).

**Acknowledgments:** The authors are grateful to the Lantmännen Research Foundation for providing the funding for this project. We also thank the University of Auckland, New Zealand for allowing us to use their nanoindentation instrument for this research.

**Conflicts of Interest:** The authors declare no conflict of interest.

## References

1. Das, O.; Hedenqvist, M.S. Self-Reinforced Gluten Polymers: A Step towards a True Biocomposite. *Open Access Government*, May 2018; 178.
2. Irissin-Mangata, J.; Bauduin, G.; Boutevi, B. Bilayer films composed of wheat gluten film and UV-cured coating: Water vapor permeability and other functional properties. *Polym. Bull.* **2000**, *44*, 409–416. [[CrossRef](#)]
3. Capezza, A.J. *Novel Superabsorbent Materials Obtained from Plant Proteins—A Report*; Department of Plant Breeding, Swedish University of Agricultural Sciences: Alnarp, Sweden, 2017; pp. 1–54.
4. Cho, S.W.; Blomfeldt, T.O.; Halonen, H.; Gällstedt, M.; Hedenqvist, M.S. Wheat gluten-laminated paperboard with improved moisture barrier properties: A new concept using a plasticizer (Glycerol) containing a hydrophobic component (Oleic Acid). *Int. J. Polym. Sci.* **2012**, *2012*, 454359. [[CrossRef](#)]
5. Gennadios, A.; Weller, C.L.; Testin, R.F. Modification of physical and barrier properties of edible wheat gluten-based films. *Cereal Chem.* **1993**, *70*, 426–429.
6. Guilbert, S.; Seow, C.C.; Teng, T.T.; Quah, C.H. *Food Preservation and Moisture Control*; Elsevier Applied Science: London, UK, 1988; pp. 199–219.
7. Zhang, H.; Mittal, G. Biodegradable protein-based films from plant resources: A review. *Environ. Prog. Sustain. Energy* **2010**, *29*, 203–220. [[CrossRef](#)]
8. Gontard, N.; Marchesseau, S.; Cuq, J.L.; Guilbert, S. Water vapour permeability of edible bilayer films of wheat gluten and lipids. *Int. J. Food Sci. Technol.* **1995**, *30*, 49–56. [[CrossRef](#)]
9. Hager, A.S.; Vallons, K.J.; Arendt, E.K. Influence of gallic acid and tannic acid on the mechanical and barrier properties of wheat gluten films. *J. Agric. Food Chem.* **2012**, *60*, 6157–6163. [[CrossRef](#)] [[PubMed](#)]
10. Hernández-Muñoz, P.; Villalobos, R.; Chiralt, A. Effect of cross-linking using aldehydes on properties of glutenin-rich films. *Food Hydrocoll.* **2004**, *18*, 403–411. [[CrossRef](#)]
11. Gennadios, A.; Weller, C.L.; Testin, R.F. Property modification of edible wheat, gluten-based films. *Trans. ASAE* **1993**, *36*, 465–470. [[CrossRef](#)]
12. Cho, S.W.; Gällstedt, M.; Hedenqvist, M.S. Properties of wheat gluten/poly (lactic acid) laminates. *J. Agric. Food Chem.* **2010**, *58*, 7344–7350. [[CrossRef](#)] [[PubMed](#)]
13. Irissin-Mangata, J.; Boutevin, B.; Bauduin, G. Bilayer films composed of wheat gluten and functionalized polyethylene: Permeability and other physical properties. *Polym. Bull.* **1999**, *43*, 441–448. [[CrossRef](#)]

14. Gontard, N.; Duchez, C.; Cuq, J.L.; Guilbert, S. Edible composite films of wheat gluten and lipids: Water vapour permeability and other physical properties. *Int. J. Food Sci. Technol.* **1994**, *29*, 39–50. [[CrossRef](#)]
15. Fabra, M.J.; Lopez-Rubio, A.; Lagaron, J.M. Effect of the film-processing conditions, relative humidity and ageing on wheat gluten films coated with electrospun polyhydryalkanoate. *Food Hydrocoll.* **2015**, *44*, 292–299. [[CrossRef](#)]
16. Micard, V.; Belamri, R.; Morel, M.H.; Guilbert, S. Properties of chemically and physically treated wheat gluten films. *J. Agric. Food Chem.* **2000**, *48*, 2948–2953. [[CrossRef](#)] [[PubMed](#)]
17. Iwata, T. Biodegradable and bio-based polymers: Future prospects of eco-friendly plastics. *Angew. Chem. Int. Ed.* **2015**, *54*, 3210–3215. [[CrossRef](#)] [[PubMed](#)]
18. Alaerts, L.; Augustinus, M.; Van Acker, K. Impact of Bio-Based Plastics on Current Recycling of Plastics. *Sustainability* **2018**, *10*, 1487. [[CrossRef](#)]
19. Wu, Q.; Andersson, R.L.; Holgate, T.; Johansson, E.; Gedde, U.W.; Olsson, R.T.; Hedenqvist, M.S. Highly porous flame-retardant and sustainable biofoams based on wheat gluten and in situ polymerized silica. *J. Mater. Chem. A* **2014**, *2*, 20996–21009. [[CrossRef](#)]
20. Wu, Q.; Yu, S.; Kollert, M.; Mtimet, M.; Roth, S.V.; Gedde, U.W.; Johansson, E.; Olsson, R.T.; Hedenqvist, M.S. Highly absorbing antimicrobial biofoams based on wheat gluten and its biohybrids. *ACS Sustain. Chem. Eng.* **2016**, *4*, 2395–2404. [[CrossRef](#)]
21. *ASTM D638-14 Standard Test Method for Tensile Properties of Plastics*; ASTM International: West Conshohocken, PA, USA, 2014.
22. Das, O.; Sarmah, A.K.; Bhattacharyya, D. Nanoindentation assisted analysis of biochar added biocomposites. *Compos. Part B Eng.* **2016**, *91*, 219–227. [[CrossRef](#)]
23. *ASTM D1653-13 Standard Test Methods for Water Vapor Transmission of Organic Coating Films*; ASTM International: West Conshohocken, PA, USA, 2013.
24. Das, O.; Bhattacharyya, D.; Hui, D.; Lau, K.T. Mechanical and flammability characterisations of biochar/polypropylene biocomposites. *Compos. Part B Eng.* **2016**, *106*, 120–128. [[CrossRef](#)]
25. Ali, Y.; Ghorpade, V.M.; Hanna, M.A. Properties of thermally-treated wheat gluten films. *Ind. Crop Prod.* **1997**, *6*, 177–184. [[CrossRef](#)]
26. Jansens, K. Gluten Cross-Linking and its Importance for the Mechanical Properties of Rigid Wheat Gluten Bioplastics. Ph.D. Thesis, KU Leuven, Leuven, Belgium, February 2013.
27. Hendrix, J.A.; Booi, M.; Frentzen, Y.H. Depolymerization of Polyamides. U.S. Patent 5,668,277, 16 September 1997.
28. Young's Modulus of Elasticity for Metals and Alloys. Available online: [https://www.engineeringtoolbox.com/young-modulus-d\\_773.html](https://www.engineeringtoolbox.com/young-modulus-d_773.html) (accessed on 14 September 2018).
29. Day, L.; Augustin, M.A.; Batey, I.L.; Wrigley, C.W. Wheat-gluten uses and industry needs. *Trend Food Sci. Technol.* **2006**, *17*, 82–90. [[CrossRef](#)]
30. Das, O.; Sarmah, A.K.; Bhattacharyya, D. Structure–mechanics property relationship of waste derived biochars. *Sci. Total Environ.* **2015**, *538*, 611–620. [[CrossRef](#)] [[PubMed](#)]
31. Das, O.; Bhattacharyya, D. Development of Polymeric Biocomposites: Particulate Incorporation, Interphase Generation and Evaluation by Nanoindentation. In *Interface/Interphase in Polymer Nanocomposites*; Netravali, A.N., Mittal, K.L., Eds.; John Wiley & Sons: Hoboken, NJ, USA, 2016; pp. 333–374.
32. Ni, W.; Cheng, Y.T.; Lukitsch, M.J.; Weiner, A.M.; Lev, L.C.; Grummon, D.S. Effects of the ratio of hardness to Young's modulus on the friction and wear behavior of bilayer coatings. *Appl. Phys. Lett.* **2004**, *85*, 4028–4030. [[CrossRef](#)]
33. Rusu, E.; Drobot, M.; Barboiu, V. Structural investigations of amines treated polyester thin films by FTIR-ATR spectroscopy. *J. Optoelectron. Adv. Mater.* **2008**, *10*, 377–381.
34. Noel, S.; Liberelle, B.; Robitaille, L.; De Crescenzo, G. Quantification of primary amine groups available for subsequent biofunctionalization of polymer surfaces. *Bioconj. Chem.* **2011**, *22*, 1690–1699. [[CrossRef](#)] [[PubMed](#)]

